

Effect of canine mesenchymal stromal cells overexpressing heme oxygenase-1 in spinal cord injury

Seung Hoon Lee, Yongsun Kim, Daeun Rhew, Ahyoung Kim, Kwang Rae Jo, Yongseok Yoon, Kyeung Uk Choi, Taeseong Jung, Wan Hee Kim, Oh-Kyeong Kweon*

BK21 PLUS Program for Creative Veterinary Science Research, Research Institute for Veterinary Science and College of Veterinary Medicine, Seoul National University, Seoul 08872, Korea

Heme oxygenase-1 (HO-1) is a stress-responsive enzyme that modulates the immune response and oxidative stress associated with spinal cord injury (SCI). This study aimed to investigate neuronal regeneration via transplantation of mesenchymal stromal cells (MSCs) overexpressing HO-1. Canine MSCs overexpressing HO-1 were generated by using a lentivirus packaging protocol. Eight beagle dogs with experimentally-induced SCI were divided into GFP-labeled MSC (MSC-GFP) and HO-1-overexpressing MSC (MSC-HO-1) groups. MSCs (1×10^7 cells) were transplanted at 1 week after SCI. Spinal cords were harvested 8 weeks after transplantation, after which histopathological, immunofluorescence, and western blot analyses were performed. The MSC-HO-1 group showed significantly improved functional recovery at 7 weeks after transplantation. Histopathological results showed fibrotic changes and microglial cell infiltration were significantly decreased in the MSC-HO-1 group. Immunohistochemical (IHC) results showed significantly increased expression levels of HO-1 and neuronal markers in the MSC-HO-1 group. Western blot results showed significantly decreased expression of tumor necrosis factor-alpha, interleukin-6, cyclooxygenase 2, phosphorylated-signal transducer and activator of transcription 3, and galactosylceramidase in the MSC-HO-1 group, while expression levels of glial fibrillary acidic protein, β 3-tubulin, neurofilament medium, and neuronal nuclear antigen were similar to those observed in IHC results. Our results demonstrate that functional recovery after SCI can be promoted to a greater extent by transplantation of HO-1-overexpressing MSCs than by normal MSCs.

Keywords: heme oxygenase-1, mesenchymal stromal cells, spinal cord injuries

Introduction

Primary mechanical damage due to spinal cord injury (SCI) results in local hemorrhage, edema, and tissue necrosis. Subsequently, secondary events, including ischemia, anoxia, inflammation, apoptosis, and free radical production, occur over a period of hours to days post-SCI. Of these, oxidative stress caused by reactive oxygen species (ROS) is the major contributor to secondary damage [18,27]. Extravasated fluid from hemorrhages causes hematoma formation, and the resulting exposure of the injured spinal cord to hemoglobin and other products leads to the generation of free radicals. Infiltrating neutrophils and macrophages are additional sources of ROS. Production of free radicals thus exacerbates the SCI [2,28].

Heme oxygenase-1 (HO-1) is an endogenous enzyme that degrades heme to iron, biliverdin, and carbon monoxide; these products contribute to strong oxidative efficacy, anti-inflammatory

effects, modulation of the immune response, and maintenance of microcirculation [9,19]. Activation of HO-1 demonstrates the endogenous defense mechanism utilized by cells to reduce inflammation and tissue damage [20]. Therefore, neuronal tissue damage caused by secondary oxidative stress in SCI could be reduced by the actions of HO-1.

Previous studies have shown that transplantation of mesenchymal stromal cells (MSCs) can reduce secondary damage and improve functional recovery after SCI [23,31]. Genetically modified MSCs have been used to deliver genes encoding growth factors such as brain derived neurotrophic factor, nerve growth factor, and neurotrophin-3 [6,17,30]. However, most transplanted cells died within the first few days post-transplant due to oxidative stress, hypoxia, and immune response [32]. Furthermore, improvement of functional recovery after MSC transplantation in a canine SCI model was limited to non-weight bearing conditions [15,22,26]. Thus, to improve

Received 23 Mar. 2016, Revised 4 Jul. 2016, Accepted 26 Aug. 2016

*Corresponding author: Tel: +82-2-880-1248; Fax: +82-2-888-2866; E-mail: ohkweon@snu.ac.kr

Journal of Veterinary Science · © 2017 The Korean Society of Veterinary Science. All Rights Reserved.

This is an Open Access article distributed under the terms of the Creative Commons Attribution Non-Commercial License (<http://creativecommons.org/licenses/by-nc/4.0>) which permits unrestricted non-commercial use, distribution, and reproduction in any medium, provided the original work is properly cited.

pISSN 1229-845X

eISSN 1976-555X

functional recovery, there is a need to develop additional methods that will better utilize MSCs in SCI treatment.

Therefore, in the present study, we generated MSCs that overexpressed canine HO-1 (MSC-HO-1) and evaluated their effectiveness in a canine SCI model. We determined the feasibility of using MSC-HO-1 by comparing its anti-inflammatory activity, neuronal regeneration, and functional recovery effects with those of normal MSCs.

Materials and Methods

In vitro procedures

Isolation and culture of canine adipose tissue-derived mesenchymal stromal cells: Canine adipose tissue-derived MSCs (cADMSCs) were obtained by applying the methods described previously [15]. Briefly, adipose tissue was aseptically collected from gluteal subcutaneous fat of 2-year-old beagle dogs under general anesthesia. All experimental procedures involving animals were approved by the Institutional Animal Care and Use Committee of Seoul National University (SNU-141231-1), Korea. The fat tissue was washed with phosphate-buffered saline (PBS), and digested with collagenase type I (1 mg/mL; Sigma-Aldrich, USA) for 2 h at 37°C. The samples were then washed with PBS and centrifuged at 300 × g for 10 min. The pellet (*i.e.*, the stromal vascular fraction) was resuspended, filtered through a 100 µm nylon mesh, and incubated in Dulbecco's modified Eagle's medium (DMEM) with 10% fetal bovine serum (FBS; Gibco-BRL, USA) at 37°C with 5% humidified CO₂. The medium was changed at 48 h intervals until cellular confluence. After the cells reached 90% confluence, they were either trypsinized and stored in liquid nitrogen or subcultured. The cells were used for subsequent experiments at passage 3. The cADMSCs used in this study were characterized previously [13].

Cloning of canine HO-1: We cloned the canine HO-1 gene with reference to the gene database in PubMed. The pPACK Packaging Plasmid Mix (System Biosciences, USA) was used for lentiviral packaging. Briefly, the gene encoding Flag-tagged HO-1 was amplified from cDNA isolated from canine peripheral blood using Phusion DNA Polymerases (Thermo Scientific, USA), and a canine HO-1-specific primer set was inserted into a pCDH-EF1-MCS-pA-PGK-copGFP-T2A-Puro vector by using the restriction enzymes EcoRI and BamHI (System Biosciences).

Generation of lentiviruses containing canine HO-1 and/or green fluorescent protein (GFP), and their transfection into cADMSCs: HEK293T cells (Thermo Scientific) were maintained in 10% FBS and 1% penicillin/streptomycin in DMEM at 37°C and 5% CO₂. Twenty-four hours before transfection, 4 × 10⁶ HEK293 cells were seeded onto a 100 mm dish. The following day, 20 µL of a lentiviral packaging mix (System Biosciences) encoding the viral proteins Gag-Pol, Rev,

and VSV-G, as well as 2 µg of lentiviral transgene plasmids, were transfected into cells for lentivirus production by using TurboFect (Thermo Scientific). GFP-labeled HO-1-expressing virus particles and GFP-expressing virus particles were collected and transduced into cADMSCs at passage 1. After the cADMSCs reached 90% confluence, the selection step was performed by using puromycin (3 µg/mL, Gibco-BRL). Approximately 40% of cells were successfully transduced after the puromycin selection step. The cADMSCs were then subcultured, and passage 3 cells were used for the subsequent experiments. All experimental procedures were performed in accordance with Seoul National University Institutional Biosafety Committee (SNUIBC) requirements (SNUIBC-R150716-1-1).

Viability of overexpressed MSCs: After MSCs reached 90% confluence, they were trypsinized and cell viability was measured by using the AO/PI cell viability kit (F23001; Logos Biosystems, USA) and a dual fluorescence cell counter (Luna-FL; Logos Biosystems). Cell viability was examined repeatedly (4 times).

Western blot analysis: The cADMSCs, GFP-labeled MSC (MSC-GFP), and MSC-HO-1 were prepared for western blot analysis as previously described [22]. Briefly The cell lysates were cleared and protein concentrations were determined by using the Bradford method [4]. Equal sample amounts (20 µg) were resolved by electrophoresis on 10% sodium dodecyl sulfate polyacrylamide gels and then transferred to polyvinylidene fluoride membranes. Membrane blots were washed with TBST (10 mM Tris-HCl, pH 7.6, 150 mM NaCl, 0.05% Tween-20), blocked with 5% skim milk for 1 h, and incubated with the appropriate primary antibodies at the recommended dilutions. The membranes were then washed, and the primary antibodies were detected with goat anti-rabbit IgG or goat anti-mouse IgG conjugated to horseradish peroxidase. The secondary antibodies were diluted at 1:2,000. Bands were visualized by using enhanced chemiluminescence (Amersham Pharmacia Biotech, UK). The primary antibodies used and their final dilutions are anti-actin (Sigma-Aldrich) at 1:1,000, anti-heme oxygenase 1 (Abcam, UK) at 1:2,000, and anti-GFP (Thermo Scientific) at 1:1,000. Western blot analysis was performed 4 times for each sample, and all methods were performed in triplicate.

Total antioxidant capacity assay: A total antioxidant capacity assay kit (OxiSelect; Cell Biolabs, USA) was used to measure the antioxidant capacity of the cell extract. Samples were prepared and dispensed into a 96-well plate, and the reaction buffer was added to each well and mixed. The copper ion reagent was dispensed into each well to start the reaction and the mixture was incubated for 5 min. Finally, the stop solution was added to end the reaction. The absorbance values were proportional to the total reductive capacity of the sample. Results are expressed as uric acid equivalents (UAE). To determine the UAE (mM) of the sample, a standard curve, $y = 0.462x + 0.061$

($R^2 = 0.9938$), was used. The y -value indicated absorbance, which was used to obtain the UAE (mM) that provides the same optical density at 490 nm. Antioxidant capacity detection was examined repeatedly (4 times).

***In vivo* procedures**

Induction of spinal cord injury: Eight healthy female beagle dogs, weighing an average of 10.61 ± 1.91 kg, were used for the present study. All dogs were judged to be in good health, neurologically normal, and were assigned their own admission number from the Institute of Laboratory Animal Resources, Seoul National University (SNU-150209-3). During the study, all dogs were cared for in accordance with the Animal Care and Use Guidelines of the Institute of Laboratory Animal Resources, Seoul National University, Korea. SCI was induced in each dog by the balloon compression method as previously described [15]. Briefly, the dogs were treated with intravenous cefazolin sodium (40 mg/kg) (Cefazoline; Chong Kun Dang Pharm, Korea), tramadol (4 mg/kg) (Toranzin; Samsung Pharm, Korea), zolazepam hydrochloride (5 mg/kg) (Zoletil 50; Virbac, France), and subcutaneous atropine sulfate (0.05 mg/kg) (Atropine; Jeil Pharmaceutical, Korea). Anesthesia was maintained with 2% isoflurane inhalation (Aerrane; Ilsung Pharmaceuticals, Korea) in oxygen. The anesthetic monitor Datex-Ohmeda (Microvitec Display, UK) was used to monitor physiological parameters, including rectal temperature, oxygen saturation, end tidal CO_2 , and pulse rate, during anesthesia. Hemilaminectomy was performed at the fourth lumbar segment (L4). A 3-French embolectomy catheter (SORIN Biomedica, Italy) was inserted into the hole at L4, after which a balloon catheter was advanced under fluoroscopic guidance at the cranial margin of the first lumbar segment (L1) and inflated at that region with 50 $\mu\text{L}/\text{kg}$ of contrast agent (Omnipaque; Amersham Health, Ireland), diluted 50:50 with saline. The balloon catheter was fixed with a Chinese finger trap suture and then removed after 12 h. Following SCI induction, the soft tissues and skin were closed by using standard methods. After the operation, the dogs were bandaged and monitored in an intensive care unit. The dogs were fed a balanced diet twice a day, and, if needed, manual bladder expression was performed at least three times daily until voluntary urination was established.

Transplantation of cADMSCs into injured sites: Injection of MSC-GFP and MSC-HO-1 was performed 1 week after SCI was experimentally induced. The dogs were anesthetized by using the same methods as those described for induction of SCI. For transplantation of MSCs to the injured site, the L1 spinal cord was exposed via dorsal laminectomy. Ten million cells suspended in 150 μL of PBS were injected at the SCI site in three locations (middle of the injury site and at proximal and distal margins) to depths of 3 mm by using a 30-gauge needle.

Behavioral assessments: To evaluate the functional recovery of the hindlimbs, behavioral assessments were performed

before the operation and then weekly for 8 weeks after the operation. Each dog was videotaped from both sides and from behind for a minimum of 10 steps when walking on the floor. Dogs that could not bear weight on their hind limbs were also videotaped while being supported by holding the base of their tail. Data were recorded as Basso, Beattie, and Bresnahan (BBB) scores [3], as well as determining positions on revised Tarlov and modified Tarlov scales [24]. Two individuals blinded to the experimental conditions scored the dogs' gaits independently by viewing the videotape recordings. A mean score was calculated every week after the SCI until the end of the 9-week study period.

Histopathological and immunofluorescence analyses: The 8 experimental dogs were euthanized 8 weeks after transplantation, and the spinal cord from the eleventh thoracic segment to the third lumbar segment (L3) was extracted by dissection. Each sample was fixed in 10% sucrose/PBS at 4°C for 12 h and immersed in a 20% sucrose solution overnight at 4°C. The dura was removed with scissors, the spinal cords were embedded in optimal cutting temperature compound (Tissue-Tek; Sakura, USA), and, after being frozen, we cut the embedded spinal cords longitudinally into two sections. One-half of each section was immediately frozen with liquid nitrogen for western blot analysis, and the other half was cut into 10 μm thick sections by using a cryomicrotome. Those sections were mounted on silane-coated glass slides and stained with hematoxylin and eosin (H&E) to detect fibrosis. Histomorphometric analysis was performed on H&E-stained tissue sections at four sites in each sample by using imaging analysis software (Image J, ver. 1.47; National Institutes of Health, USA). For the immunohistochemical (IHC) analysis, primary antibodies were used and their final dilutions were as follows: HO-1 (Abcam) at 1:200, glial fibrillary acidic protein (GFAP) at 1:200, β 3-tubulin at 1:200, neurofilament medium (NF-M) at 1:1,000, neuronal nuclear antigen (NeuN) at 1:200, galactosylceramidase (GALC) at 1:500, and phosphorylated-signal transducer and activator of transcription 3 (p-STAT3) (Santa Cruz Biotechnology, USA) at 1:200 for immunofluorescence determination. The sections were fixed with 3.5% paraformaldehyde, permeabilized for 10 min with 0.1% (v/v) Triton X-100, washed, and then pre-incubated with 1% bovine serum albumin (BSA; Sigma-Aldrich) in PBS for 30 min to decrease nonspecific antibody binding. Sections were incubated with the primary antibodies overnight at 4°C and incubated for 60 min with anti-mouse or anti-rabbit secondary antibody conjugated to Alexa 647 (Abcam) at room temperature. The secondary antibodies were diluted at 1:2,000. DAPI (4,6-diamidino-2-phenylindole) was used for nuclear staining. To identify the fate and function of cADMSCs after transplantation, anti-GFP (Thermo Scientific) and other marker levels were investigated by manually counting the cells in 5 randomly selected regions of each spinal cord section. The HO-1, GFAP, β 3-tubulin, NF-M, and NeuN

marker-positive cells and the GFP-positive cells were converted to a ratio for 1,000 cells [25]. Each marker-positive cell was counted as a double-positive cell only if clearly defined borders could be detected completely around or adjacent to the entire GFP-positive nucleus. Fluorescence images were

visualized with a FluoView 300 fluorescence microscope (Olympus, Japan).

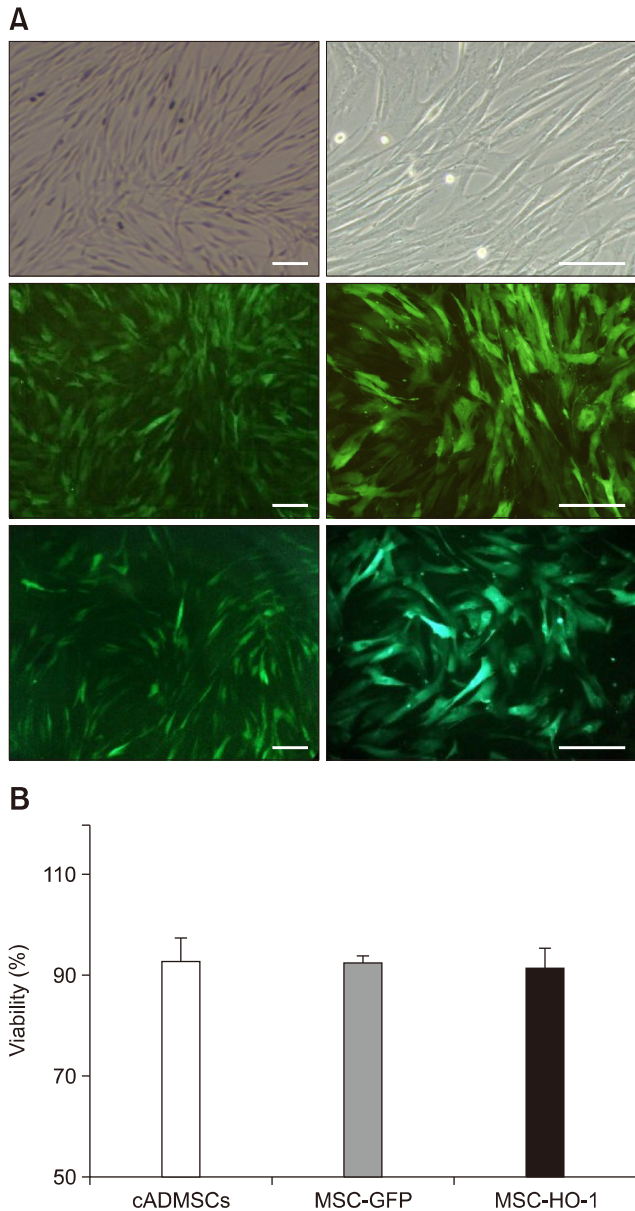


Fig. 1. Fluorescence microscopy images and cell viability results. (A) Green fluorescence protein (GFP) overexpressing cADMSCs. Top panels, cADMSC; middle panels, GFP-labeled cADMSCs (MSC-GFP); lower panels, GFP-labeled HO-1 overexpressing cADMSCs (MSC-HO-1). GFP expression was identified in MSC-GFP and MSC-HO-1 via fluorescence microscopy. Right panels are higher magnification images of left panels, respectively. (B) Cell viability of the three cell types showing no significant difference. Scale bars = 50 μ m.

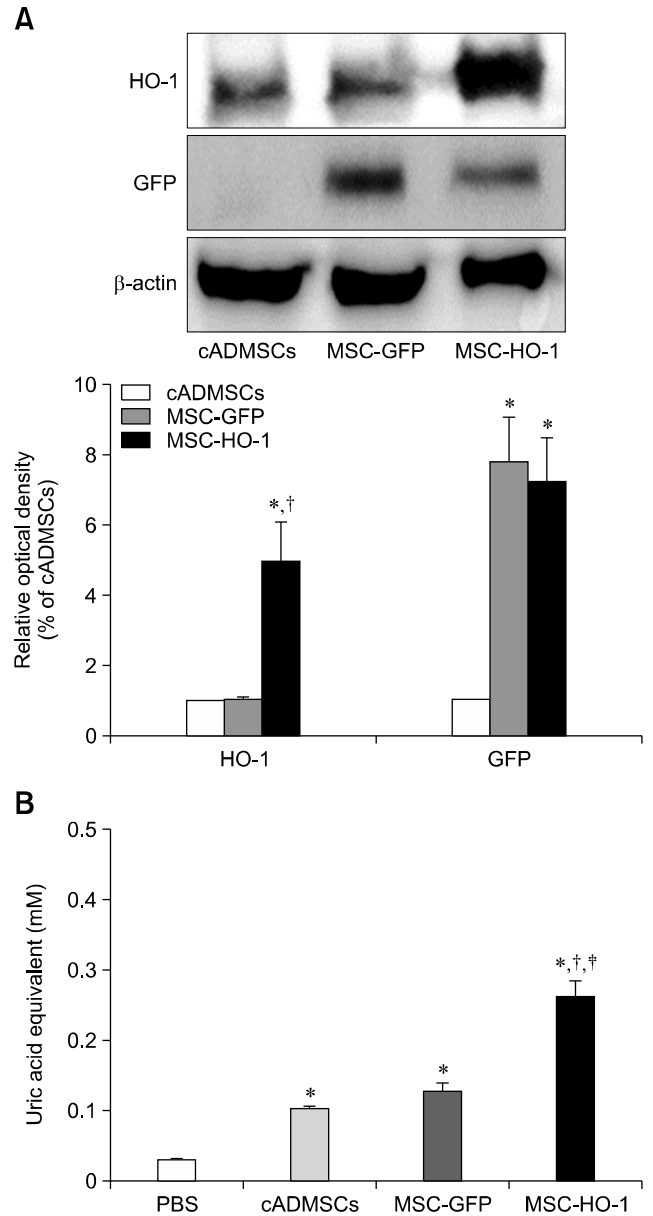


Fig. 2. Protein expression in cADMSCs overexpressing heme oxygenase 1 (HO-1) and their antioxidant effects. (A) Western blot results for cADMSCs, MSC-GFP, and MSC-HO-1. Expression of HO-1 in MSC-HO-1 was significantly higher than it was in the cADMSCs and MSC-GFP, and the MSC-GFP and MSC-HO-1 showed a significant increase in GFP expression relative to that in cADMSCs, but there was no difference between overexpressed cells (* $p < 0.05$ vs. cADMSCs, $\dagger p < 0.05$ vs. MSC-GFP). (B) Antioxidant capacity of cADMSCs, MSC-GFP, and MSC-HO-1. Uric acid equivalent level of MSC-HO-1 was significantly higher than that of the other groups. There was no difference between the cADMSCs and MSC-GFP (* $p < 0.05$ vs. PBS, $\dagger p < 0.05$ vs. cADMSCs, and $\ddagger p < 0.05$ vs. MSC-GFP).

Western blot analysis: The frozen half of each spinal cord section was used for western blot analysis. Briefly, the spinal cord tissue was washed twice with PBS and frozen at -150°C . The tissue was then homogenized by using a sonicator (three 20-second bursts; Branson Sonicator 250; Branson Ultrasonic, USA) in lysis buffer (20 mM Tris, pH 7.5, 1 mM EDTA, 1 mM EGTA, 1% Triton X-100, 1 mg/mL aprotinin, 1 mM phenylmethylsulfonyl fluoride, and 0.5 mM sodium orthovanadate) for 30 min on ice. Lysates were cleared by centrifugation (10 min at $1,500 \times g$, 4°C) and protein concentrations were determined by using the Bradford method [4]. The SDS-PAGE and electrophoretic transfer procedures were the same as those performed *in vitro*. The antibodies used and their final dilutions were as follow: anti-actin at 1:1,000, HO-1 at 1:2,000, NF-M at 1:5,000, NeuN (Abcam) at 1:1,000, anti-GFP at 1:1,000, GFAP at 1:1,000, β 3-tubulin at 1:1,000, tumor necrosis factor alpha at 1:200, interleukin-6 (IL-6) at 1:1,000, cyclooxygenase 2 (COX2) at 1:1,000, p-STAT3 at 1:1,000, and GALC (Santa Cruz Biotechnology) at 1:1,000. The primary antibodies were detected with goat anti-rabbit IgG or goat anti-mouse IgG conjugated to horseradish peroxidase. The secondary antibodies were diluted at 1:2,000. The western blot analysis was performed 4 times for each sample ($n = 8$), and all methods were performed in triplicate.

Statistical analysis: In all quantification procedures, observers were blinded to the nature of the experimental manipulation. Data are presented as medians and quartiles. Statistical analysis was performed by using a commercially available statistical software program (SPSS Statistics, ver. 21.0; IBM, USA). In all experiments with *in vitro* procedures, Kruskal-Wallis tests were followed by Mann-Whitney *U* tests in order to compare the

three groups. For the *in vivo* experiments, Mann-Whitney *U* tests were used to compare results between the two groups. A *p* value of < 0.05 was considered significant.

Results

Cell viability and protein expression in cADMSCs overexpressing HO-1

The MSC-GFP and MSC-HO-1 expressed green fluorescence when viewed through a fluorescence microscope (panel A in Fig. 1). Cell viabilities of cADMSCs, MSC-GFP, and MSC-HO-1 were $92.79 \pm 4.61\%$, $92.55 \pm 1.32\%$, and $91.53 \pm 3.25\%$, respectively. No significant difference in viability was detected among the MSCs (panel B in Fig. 1). Protein expression of HO-1 in MSC-HO-1 was significantly higher than those in the cADMSCs and MSC-GFP. Furthermore, the MSC-GFP and MSC-HO-1 showed a significant increase in GFP expression compared to that in the cADMSCs ($p < 0.05$); however, no difference was detected between the MSC-GFP and MSC-HO-1 (panel A in Fig. 2). The total antioxidant capacity of MSC-HO-1 was significantly higher than that of the other MSCs; however, there was no difference between the cADMSCs and MSC-GFP (panel B in Fig. 2) ($p < 0.05$).

Behavioral observations

After induction of SCI, all experimental dogs showed complete pelvic limb paralysis, with BBB scores of 21 prior to SCI and 0 after SCI. BBB scores were obtained every week until 8 weeks after transplantation. The BBB scores of the MSC-GFP and MSC-HO-1 groups gradually increased during the study period, but the rate of improvement decreased at 5 weeks after

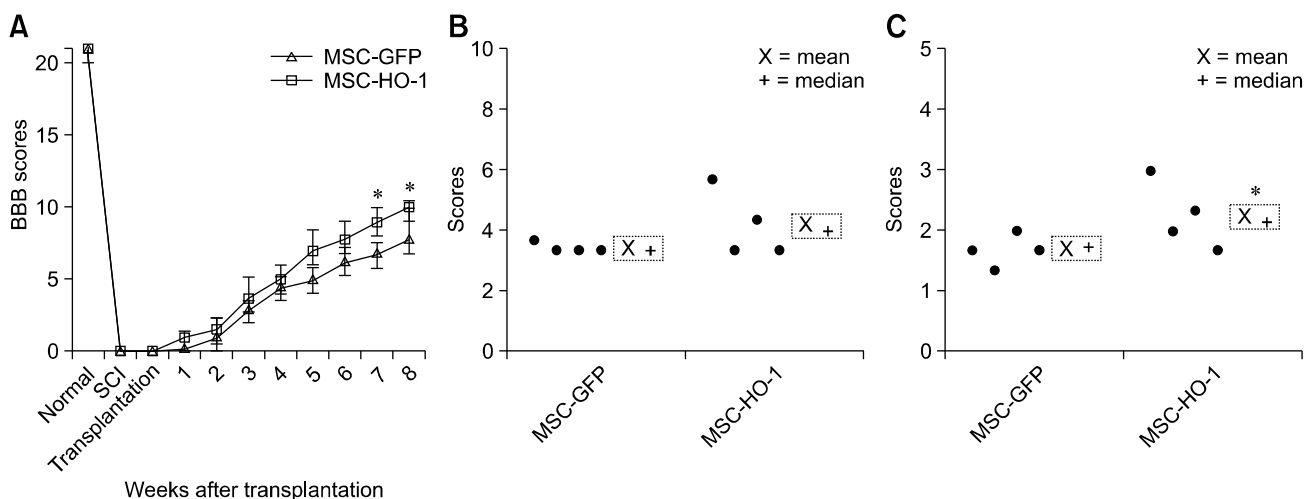


Fig. 3. Behavioral analysis results using Basso, Beattie, and Bresnahan (BBB) scores and Tarlov scales. (A) BBB scores before and during the 8 weeks after transplantation. Post-transplantation, the BBB scores of the MSC-HO-1 group were significantly improved at 7 and 8 weeks after transplantation compared with the GFP-labeled cADMSCs (MSC-GFP) scores ($*p < 0.05$). Hindlimb locomotion at 8 weeks after transplantation were determined by two grading system: (B) revised Tarlov scales and (C) modified Tarlov scales. Higher motor function recovery was indicated in the MSC-HO-1 group than the MSC-GFP group ($*p < 0.05$).

transplantation. However, compared to the MSC-GFP group score, the BBB score of the MSC-HO-1 group significantly improved at 7 weeks after transplantation ($p < 0.05$) (panel A in Fig. 3). Improvement in hindlimb function in the MSC-GFP group presented as slight or extensive movement of joints with an inability of the dogs to bear their own weight. Two dogs in the MSC-HO-1 group were able to support their body weight occasionally. To evaluate the behaviors qualitatively, we used revised and modified Tarlov scales and detected significantly higher motor recovery in the MSC-HO-1 group than in the MSC-GFP group ($p < 0.05$) (panels B and C in Fig. 3).

Histopathological and immunohistochemical analyses

Fibrotic and atrophic changes in the injured regions were detected in both groups at 8 weeks after transplantation. The sizes of the injured regions (cm) in the MSC-GFP and MSC-HO-1 groups were 1.50 ± 0.22 and 1.43 ± 0.28 , respectively, and there was no significant difference between them. Histopathological analysis with H&E staining showed pathological changes in the parenchyma. Under low-power field viewing, a reduction in fibrotic changes was observed in the MSC-HO-1 group when compared to that in the MSC-GFP group. Under high-power field viewing, aspects such as hemorrhage, fibroblast-like cell proliferation, and infiltration of microglial cells into the injured region were also observed to be reduced in the MSC-HO-1 group. Based on quantification of fibrotic tissue by examining H&E staining, significant differences were observed between the two groups ($p < 0.05$) (Fig. 4).

IHC analysis revealed that expression levels of HO-1, β 3-tubulin, NF-M, and NeuN were higher in the MSC-HO-1 group than in the MSC-GFP group, whereas those of GFAP, GALC, and p-STAT3 were lower in the MSC-HO-1 group than in the MSC-GFP group. These differences between the two groups were found to be significant (panel B in Fig. 5) ($p < 0.05$), but GFP expression showed no significant difference between the groups (panel C in Fig. 5), even though transplanted cells of both groups expressed GFP. The markers of HO-1 and neural cells were expressed as a red color. Panel D in Fig. 5 presents a comparison of the origins of HO-1 and neural cells in injured sites, whether from implanted MSCs or endogenous host cells. The expression rates of most neural cell markers of endogenous origin were significantly higher than those of transplanted cell origin in both groups ($p < 0.05$). However, the expression rate of the HO-1 marker of transplanted cells origin was significantly higher in the MSC-HO-1 group than in the MSC-GFP group (panels B–D in Fig. 5).

Western blot analysis

Western blot results showed the expression of HO-1 in the MSC-HO-1 group to be significantly higher than that in the

MSC-GFP group ($p < 0.01$); however, GFP expression was not different between the groups (Fig. 6). The inflammatory markers IL-6, COX2, p-STAT3, and GALC showed significantly decreased expressions in the MSC-HO-1 group compared to those in the MSC-GFP group ($p < 0.05$). The results of the western blot analysis of neuronal cell markers GFAP, β 3-tubulin, NF-M, and NeuN were similar to the results obtained via IHC analysis (*cf.*, Figs. 5 and 6).

Discussion

The results of the present study demonstrate the improved

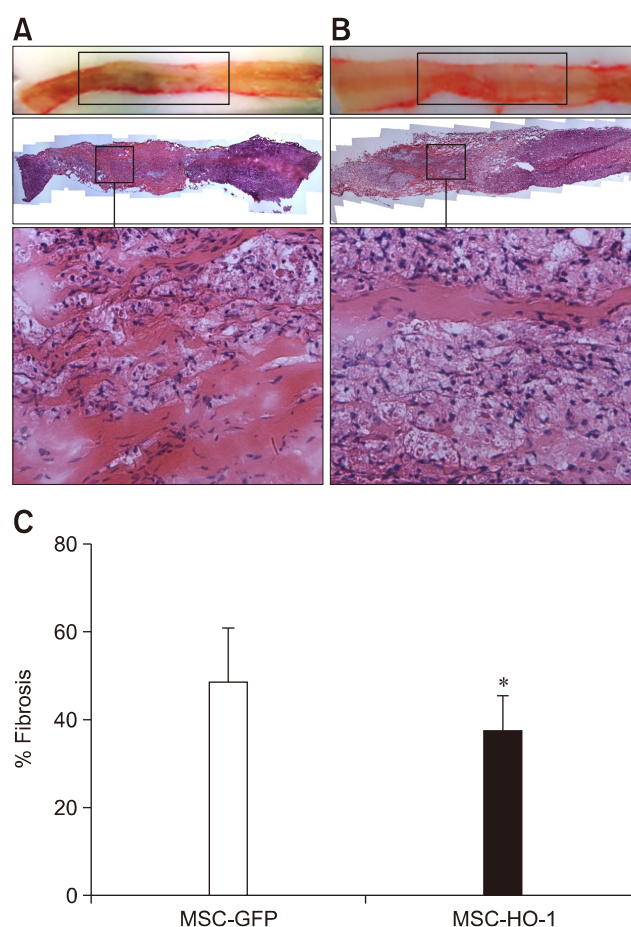


Fig. 4. Histopathological analysis with H&E staining. Histological analysis of spinal cord lesions stained with H&E. (A) MSC-GFP group; upon magnification of the injury epicenter, fibroblast-like cell proliferation was detected. (B) MSC-HO-1 group; spinal cord lesion was limited to the compression region and a greater reduction in fibrotic changes was observed compared with those in the MSC-GFP group. Also, upon magnification, a reduction in fibroblast-like cell proliferation was observed. (C) Quantification of fibrotic tissue was showed significant difference between groups ($*p < 0.05$). 40 \times (top panels of A and B), 200 \times (bottom panels of A and B; enlargements of squares of the middle panels).

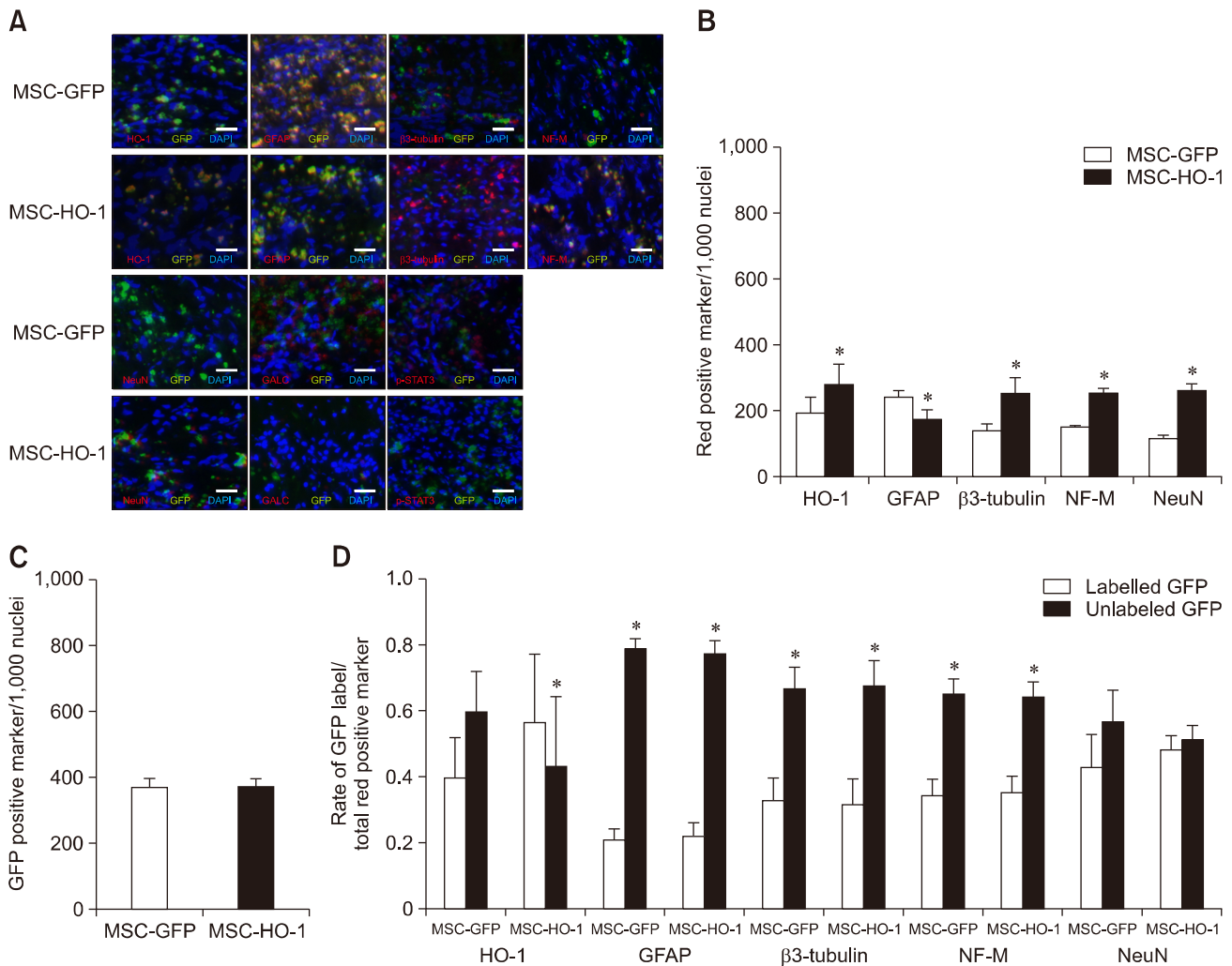


Fig. 5. Immunohistochemical assessments. (A) Immunofluorescence staining at 8 weeks after transplantation. Injured spinal cord lesions were immunostained for heme oxygenase 1 (HO-1), glial fibrillary acidic protein (GFAP), β3-tubulin, neurofilament M (NF-M), neuronal nuclear antigen (NeuN), galactosylceramidase (GALC), and phosphorylated-signal transducer and activator of transcription 3 (p-STAT3; red); transplanted cells (green fluorescent protein [GFP]); each nucleus was stained with DAPI (blue). (B), (C), and (D) showed quantification of immunostaining results. (B) Expression of red positive markers of antibodies. Expressions of the HO-1, β3-tubulin, NF-M, and NeuN were higher in the MSC-HO-1 group than MSC-GFP group, and expression of GFAP was adversely affected. The number of transplanted cells expressing GFP was not different between the two groups ($*p < 0.05$). (C) GFP expression shows no difference between the groups. (D) Comparison of the origins of HO-1 and neural cells in the injured site, whether from implanted MSCs or endogenous host cells. The expression of most neural cell markers from endogenous origins (not GFP labeled) were significantly higher than those of transplanted cells origins (GFP labeled) in both groups ($*p < 0.05$). However, expression rate of HO-1 marker from transplanted cells origins was significantly higher than that from endogenous origin cells in the MSC-HO-1 group ($*p < 0.05$). Scale bars = 50 μm.

anti-inflammatory and neuronal regeneration effects and the improved recovery of hindlimb function owing to transplantation of MSCs overexpressing HO-1, as compared to that observed with transplantation of normal cADMSCs in a canine model of SCI. Therapeutic applications of genetically modified MSCs in SCI have been reported previously [16,21,30], but most of them were related to neurotropic factors or growth factors, which were aimed at continuous secretion of the factors that stimulate axonal growth and replacement of neurons throughout the

lesion area [6,17,30]. In this study, treatment with MSC-HO-1 was designed to be a means to manifest antioxidant and anti-inflammatory effects to prevent further aggravation of SCI. In theory, if more cells survive in the lesion, that would provide a favorable environment for the ingrowth of endogenous neuronal cells. In the present study, overexpression of HO-1 was confirmed by gene and protein expression assays, and the MSC-HO-1 showed a higher antioxidative capacity than the cADMSCs, without any difference in cell viability. Modification

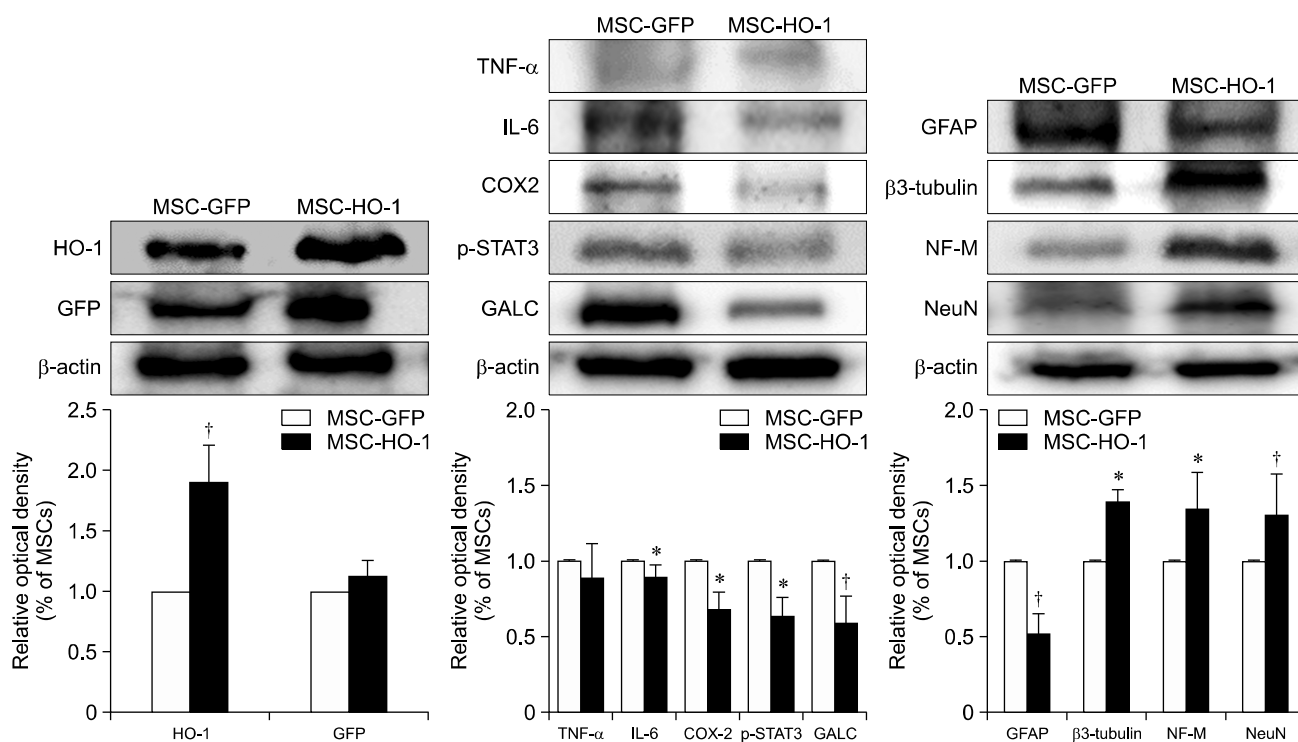


Fig. 6. Western blot analysis. Protein expressions at 8 weeks after transplantation were evaluated by western blotting. Overexpression markers, heme oxygenase 1 (HO-1) and green fluorescent protein (GFP); inflammatory markers, tumor necrosis factor- α (TNF- α), interleukin-6 (IL-6), cyclooxygenase 2 (COX2), phosphorylated-signal transducer and activator of transcription 3 (p-STAT3), and GALC; neuronal markers, glial fibrillary acidic protein (GFAP), β 3-tubulin, NF-M, and neuronal nuclear antigen (NeuN). Data presented as means \pm SE of three independent experiments. The graph and bars depict means \pm SE of four dogs per group, as determined by observed densitometry relative to β -actin (* p < 0.05, † p < 0.001).

of the HO-1 gene did not influence the original function of the cADMSCs [29,34].

Previous studies have shown that transplantation of MSCs after SCI could ameliorate the clinical outcome. However, the hindlimbs of dog in the treatment group were unable to support their body weight, and the negative control group showed only slight movement of hindlimb joints [1,10,14,22,23,26]. In the present study, for ethical reasons, we reduced the required number of animals and the negative control group was omitted. The functional recovery in the MSC-GFP group showed similar results to those of previous studies, but transplantation of MSC-HO-1 resulted in further improvement of functional recovery, mainly related to MSC-HO-1 treated dogs being able to support their body weight. Peak inflammation was observed at 1 week after SCI and transplantation of MSCs at that time showed better results than that observed at 3 days and 2 weeks after SCI [22]. In the present study, inflammation markers were expressed at significantly lower levels in the MSC-HO-1 group, and the low expression of inflammation markers in the MSC-HO-1 group can be attributed to the anti-inflammatory effects of HO-1 [5,22,31].

The environment of an injured spinal cord induces endogenous

or exogenous stem cell lineages to differentiate into astrocytes and oligodendrocytes [5,26]. The quantitative histological analyses in the present study revealed that p-STAT3 and GALC expression levels were significantly lower in the MSC-HO-1 group than in the MSC-GFP group. Expression of p-STAT3 is induced by inflammatory cytokine signaling associated with IL-6 in spinal microglia, and it regulates astrogliosis and scar formation after SCI [8,23]. In the present study, GALC, the mature oligodendrocyte marker, exhibited particularly low expression and the expression of GFAP, a reactive astrocyte marker, was also decreased in the MSC-HO-1 group. These results indicate that MSC-HO-1 could inhibit astrogliosis and scar formation processes.

The strong antioxidative, anti-inflammatory, and antiapoptotic effects of HO-1 can prevent secondary events that occur after SCI by degrading heme into biliverdin, carbon monoxide (CO), and iron, which leads to an enhancement of functional recovery after SCI [9,19,35]. Our previous study demonstrated the antioxidative effect of cADMSCs by measuring the levels of oxidative metabolites (3-nitrotyrosine, 4-hydroxynonenal, and protein oxidation-derived protein carbonyls) in the injured sites 1 week after SCI [12]. Those results suggested that MSC-HO-1

might play an important role in anti-oxidation. The present study did not evaluate oxidative markers in the injured lesions because the markers would be expressed at an earlier time after SCI than sample harvest time of the present study.

Our results showed significantly higher expressions of the immature neuronal marker β 3-tubulin, the motor neuron marker NF-M, and the neuronal biomarker NeuN in the MSC-HO-1 group than in the MSC-GFP group. In our IHC results, free GFP expression indicated the intrinsic expression of these factors, and the labeled-GFP expression indicated the exogenous manifestations of these factors. Most of the neuronal markers were shown to be of endogenous origin. Previous studies have shown that HO-1 is an endogenous enzyme that has cytoprotective and antioxidative roles in SCI [9,33]. According to the results of the present study, the MSC-GFP group exhibited endogenous HO-1 expression, but the MSC-HO-1 group exhibited more exogenous than endogenous HO-1 expression. Moreover, the expression of the exogenous HO-1 in the MSC-HO-1 group was significantly greater than that in the MSC-GFP group. Death of most transplanted MSCs occurs as a result of oxidative stress, immune response, and hypoxia within a few days of transplantation [7,32]; however, our results suggest that the transplanted MSC-HO-1 survived and continued to express HO-1 in the injured site for 8 weeks.

There are few possible explanations for the improvements in functional recovery, anti-inflammatory activity, and neuronal regeneration observed in the present study after transplantation of MSC-HO-1. Transplanted MSCs are engrafted to become new neurons, or they act as a paracrine cells secreting neural growth factors [26,29].

In this study, the degree of expression of GFP showed no difference between groups whether the MSCs were overexpressing HO-1 or not. However, when vascular smooth muscle cells [36] or mesenchymal stem cells [11] overexpressing HO-1 were stressed by H₂O₂ or freeze-thawing, the proliferation rate of the cells was decreased *in vitro* compared to that in wild type cells. Thus, overexpression of HO-1 could protect cells against oxidation injury on the one hand, but the increase of HO-1 activity of cells under stress might suppress proliferation on the other hand. It has been shown that apoptosis occurs due to arrest of the G0/G1 phase by the overexpression of HO-1 [36]. As shown by *in vitro* result of the present study, proliferation rate under normal condition was not different between MSCs expressing HO-1 and normal MSCs. However, it was supposed that the number of cells expressing GFP in MSC-HO-1 group were less than that in MSC-GFP group in the implantation site but there was no difference of the degree of expression of GFP between groups. It is possible that the implanted site was unfavorable at 1 week after SCI, a period in which inflammation had peaked [22]. A great number of implanted cells would die, especially cells overexpressing HO-1, which are supposed to be more died than MSCs-GFP wild type cells. We suggest that

there might be some beneficial effect of HO-1 not only on the cells already presented at injured site but also on the transplanted cells themselves overexpressing HO-1 *in vivo*.

The results of the present study demonstrate that transplantation of MSCs overexpressing HO-1 promotes functional recovery after SCI by enhancing the anti-inflammatory and neuronal regeneration effects of MSCs. Our results suggest that the use of MSCs overexpressing HO-1 could be an effective therapeutic method for use in SCI.

Acknowledgments

This work was supported by the National Research Foundation of Korea (NRF-2015R1D1A1A01057415).

Conflict of Interest

The authors declare no conflict of interests.

References

1. **Andrews EM, Tsai SY, Johnson SC, Farrer JR, Wagner JP, Kopen GC, Kartje GL.** Human adult bone marrow-derived somatic cell therapy results in functional recovery and axonal plasticity following stroke in the rat. *Exp Neurol* 2008, **211**, 588-592.
2. **Bains M, Hall ED.** Antioxidant therapies in traumatic brain and spinal cord injury. *Biochim Biophys Acta* 2012, **1822**, 675-684.
3. **Barros Filho TEP, Molina AEIS.** Analysis of the sensitivity and reproducibility of the Basso, Beattie, Bresnahan (BBB) scale in Wistar rats. *Clinics (Sao Paulo)* 2008, **63**, 103-108.
4. **Bradford MM.** A rapid and sensitive method for the quantitation of microgram quantities of protein utilizing the principle of protein-dye binding. *Anal Biochem* 1976, **72**, 248-254.
5. **Cho SR, Kim YR, Kang HS, Yim SH, Park CI, Min YH, Lee BH, Shin JC, Lim JB.** Functional recovery after the transplantation of neurally differentiated mesenchymal stem cells derived from bone marrow in a rat model of spinal cord injury. *Cell Transplant* 2009, **18**, 1359-1368.
6. **Dougherty KD, Dreyfus CF, Black IB.** Brain-derived neurotrophic factor in astrocytes, oligodendrocytes, and microglia/macrophages after spinal cord injury. *Neurobiol Dis* 2000, **7**, 574-585.
7. **Emgård M, Hallin U, Karlsson J, Bahr BA, Brundin P, Blomgren K.** Both apoptosis and necrosis occur early after intracerebral grafting of ventral mesencephalic tissue: a role for protease activation. *J Neurochem* 2003, **86**, 1223-1232.
8. **Herrmann JE, Imura T, Song B, Qi J, Ao Y, Nguyen TK, Korsak RA, Takeda K, Akira S, Sofroniew MV.** STAT3 is a critical regulator of astrogliosis and scar formation after spinal cord injury. *J Neurosci* 2008, **28**, 7231-7243.
9. **Kanno H, Ozawa H, Dohi Y, Sekiguchi A, Igarashi K, Itoi E.** Genetic ablation of transcription repressor Bach1 reduces neural tissue damage and improves locomotor function after

- spinal cord injury in mice. *J Neurotrauma* 2009, **26**, 31-39.
10. **Keirstead HS, Nistor G, Bernal G, Totoiu M, Cloutier F, Sharp K, Steward O.** Human embryonic stem cell-derived oligodendrocyte progenitor cell transplants remyelinate and restore locomotion after spinal cord injury. *J Neurosci* 2005, **25**, 4694-4705.
 11. **Kim M, Kim Y, Lee S, Kuk M, Kim AY, Kim W, Kweon OK.** Comparison of viability and antioxidant capacity between canine adipose-derived mesenchymal stem cells and heme oxygenase-1-overexpressed cells after freeze-thawing. *J Vet Med Sci* 2016, **78**, 619-625.
 12. **Kim Y, Jo SH, Kim WH, Kweon OK.** Antioxidant and anti-inflammatory effects of intravenously injected adipose derived mesenchymal stem cells in dogs with acute spinal cord injury. *Stem Cell Res Ther* 2015, **6**, 229.
 13. **Kuk M, Kim Y, Lee SH, Kim WH, Kweon OK.** Osteogenic ability of canine adipose-derived mesenchymal stromal cell sheets in relation to culture time. *Cell Transplant* 2016, **25**, 1415-1422.
 14. **Lee SH, Kim Y, Rhew D, Kuk M, Kim M, Kim WH, Kweon OK.** Effect of the combination of mesenchymal stromal cells and chondroitinase ABC on chronic spinal cord injury. *Cytotherapy* 2015, **17**, 1374-1383.
 15. **Lim JH, Byeon YE, Ryu HH, Jeong YH, Lee YW, Kim WH, Kang KS, Kweon OK.** Transplantation of canine umbilical cord blood-derived mesenchymal stem cells in experimentally induced spinal cord injured dogs. *J Vet Sci* 2007, **8**, 275-282.
 16. **Lu P, Jones LL, Tuszynski MH.** Axon regeneration through scars and into sites of chronic spinal cord injury. *Exp Neurol* 2007, **203**, 8-21.
 17. **Lu P, Jones LL, Tuszynski MH.** BDNF-expressing marrow stromal cells support extensive axonal growth at sites of spinal cord injury. *Exp Neurol* 2005, **191**, 344-360.
 18. **Mothe AJ, Tator CH.** Review of transplantation of neural stem/progenitor cells for spinal cord injury. *Int J Dev Neurosci* 2013, **31**, 701-713.
 19. **Öllinger R, Pratschke J.** Role of heme oxygenase-1 in transplantation. *Transpl Int* 2010, **23**, 1071-1081.
 20. **Origassa CST, Câmara NOS.** Cytoprotective role of heme oxygenase-1 and heme degradation derived end products in liver injury. *World J Hepatol* 2013, **5**, 541-549.
 21. **Osaka M, Honmou O, Murakami T, Nonaka T, Houkin K, Hamada H, Kocsis JD.** Intravenous administration of mesenchymal stem cells derived from bone marrow after contusive spinal cord injury improves functional outcome. *Brain Res* 2010, **1343**, 226-235.
 22. **Park SS, Byeon YE, Ryu HH, Kang BJ, Kim Y, Kim WH, Kang KS, Han HJ, Kweon OK.** Comparison of canine umbilical cord blood-derived mesenchymal stem cell transplantation times: involvement of astrogliosis, inflammation, intracellular actin cytoskeleton pathways, and neurotrophin-3. *Cell Transplant* 2011, **20**, 1867-1880.
 23. **Park SS, Lee YJ, Lee SH, Lee D, Choi K, Kim WH, Kweon OK, Han HJ.** Functional recovery after spinal cord injury in dogs treated with a combination of Matrigel and neural-induced adipose-derived mesenchymal stem cells. *Cytotherapy* 2012, **14**, 584-597.
 24. **Rabinowitz RS, Eck JC, Harper CM Jr, Larson DR, Jimenez MA, Parisi JE, Friedman JA, Yaszemski MJ, Currier BL.** Urgent surgical decompression compared to methylprednisolone for the treatment of acute spinal cord injury: a randomized prospective study in beagle dogs. *Spine (Phila Pa 1976)* 2008, **33**, 2260-2268.
 25. **Ryu HH, Byeon YE, Park SS, Kang BJ, Seo MS, Park SB, Kim WH, Kang KS, Kweon OK.** Immunohistomorphometric analysis of transplanted umbilical cord blood-derived mesenchymal stem cells and the resulting anti-inflammatory effects on nerve regeneration of injured canine spinal cord. *Tissue Eng Regen Med* 2011, **8**, 173-182.
 26. **Ryu HH, Lim JH, Byeon YE, Park JR, Seo MS, Lee YW, Kim WH, Kang KS, Kweon OK.** Functional recovery and neural differentiation after transplantation of allogenic adipose-derived stem cells in a canine model of acute spinal cord injury. *J Vet Sci* 2009, **10**, 273-284.
 27. **Snyder EY, Teng YD.** Stem cells and spinal cord repair. *N Engl J Med* 2012, **366**, 1940-1942.
 28. **Soares MP, Marguti I, Cunha A, Larsen R.** Immunoregulatory effects of HO-1: how does it work? *Curr Opin Pharmacol* 2009, **9**, 482-489.
 29. **Tang YL, Tang Y, Zhang YC, Qian K, Shen L, Phillips MI.** Improved graft mesenchymal stem cell survival in ischemic heart with a hypoxia-regulated heme oxygenase-1 vector. *J Am Coll Cardiol* 2005, **46**, 1339-1350.
 30. **Taylor L, Jones L, Tuszynski MH, Blesch A.** Neurotrophin-3 gradients established by lentiviral gene delivery promote short-distance axonal bridging beyond cellular grafts in the injured spinal cord. *J Neurosci* 2006, **26**, 9713-9721.
 31. **Torres-Espín A, Redondo-Castro E, Hernandez J, Navarro X.** Immunosuppression of allogenic mesenchymal stem cells transplantation after spinal cord injury improves graft survival and beneficial outcomes. *J Neurotrauma* 2015, **32**, 367-380.
 32. **Uemura M, Refaat MM, Shinoyama M, Hayashi H, Hashimoto N, Takahashi J.** Matrigel supports survival and neuronal differentiation of grafted embryonic stem cell-derived neural precursor cells. *J Neurosci Res* 2010, **88**, 542-551.
 33. **Yamauchi T, Lin Y, Sharp FR, Noble-Haesslein LJ.** Hemin induces heme oxygenase-1 in spinal cord vasculature and attenuates barrier disruption and neutrophil infiltration in the injured murine spinal cord. *J Neurotrauma* 2004, **21**, 1017-1030.
 34. **Yeom HJ, Koo OJ, Yang J, Cho B, Hwang JI, Park SJ, Hurh S, Kim H, Lee EM, Ro H, Kang JI, Kim SJ, Won JK, O'Connell PJ, Kim H, Surh CD, Lee BC, Ahn C.** Generation and characterization of human heme oxygenase-1 transgenic pigs. *PLoS One* 2012, **7**, e46646.
 35. **Zhang LF, Qi J, Zuo G, Jia P, Shen X, Shao J, Kang H, Yang H, Deng L.** Osteoblast-secreted factors promote proliferation and osteogenic differentiation of bone marrow stromal cells via VEGF/heme-oxygenase-1 pathway. *PLoS One* 2014, **9**, e99946.
 36. **Zhang M, Zhang BH, Chen L, An W.** Overexpression of heme oxygenase-1 protects smooth muscle cells against oxidative injury and inhibits cell proliferation. *Cell Res* 2002, **12**, 123-132.